MR fluid damper-based smart damping systems for long steel stay cable under wind load

Hyung-Jo Jung*

Department of Civil and Environmental Engineering, Korea Advanced Institute of Science and Technology,373-1 Guseong-dong, Yuseong-gu, Daejeon 305-701, Korea

Ji-Eun Jang

University of California, Santa Babara, Santa Babara, CA 93106, USA

Kang-Min Choi and Heon-Jae Lee

Department of Civil and Environmental Engineering, Korea Advanced Institute of Science and Technology,373-1 Guseong-dong, Yuseong-gu, Daejeon 305-701, Korea

Abstract. Long steel stay cables, which are mainly used in cable-stayed bridges, are easy to vibrate because of their low inherent damping characteristics. A lot of methods for vibration reduction of stay cables have been developed, and several techniques of them have been implemented to real structures, though each has its limitations. Recently, it was reported that smart (i.e. semi-active) dampers can potentially achieve performance levels nearly the same as comparable active devices with few of the detractions. Some numerical and experimental studies on the application of smart damping systems employing an MR fluid damper, which is one of the most promising smart dampers, to a stay cable were carried out; however, most of the previous studies considered only one specific control algorithm in which they are interested. In this study, the performance verification of MR fluid damper-based smart damping systems for mitigating vibration of stay cables by considering the four commonly used semi-active control algorithms, such as the control algorithm based on Lyapunov stability theory, the maximum energy dissipation algorithm, the modulated homogeneous friction algorithm and the clipped-optimal control algorithm, is systematically carried out to find the most appropriate control strategy for the cable-damper system.

Keywords: stay cable; smart damping system; semiactive control algorithm; MR fluid damper.

1. Introduction

A smart (i.e. semi-active) damping system based on magnetorheological (MR) fluid dampers has become widely studied in the field of civil engineering because of its many attractive characteristics for use in vibration control applications. MR fluid dampers may be operated directly from small power supplies, while they are relatively inexpensive to manufacture, are less sensitive to contaminants in fluids, and have a broader operational temperature range. In addition, the dampers are characterized by

*Assistant Professor, Corresponding Author, E-mail: hjung@kaist.ac.kr

their ability to dynamically vary their properties with a minimal amount of power, and may provide reliability as well as stability. As semi-active devices such as MR fluid dampers have demonstrated promise for civil engineering applications, many studies developed a phenomenological model (Spencer, *et al*. 1997), proposed the numerous control algorithms appropriate for implementation in full-scale structures and tried new application of semi-active devices for civil engineering structures (e.g., Cho, *et al*. 2005, Choi, *et al*. 2007a, Jung, *et al*. 2007).

Recently, several studies have adopted semi-active controllers to suppress stay cable vibration. Long steel stay cables, such as are widely used in cable-stayed bridges and other cable structures, are highly susceptible to vibration caused by wind, rain and support motion due to their large flexibility, relatively small mass and extremely low inherent damping. A number of methods, such as tying multiple cables together, aerodynamic cable surface modification, and passive and active axial and transverse cable control, have been proposed and/or implemented to suppress cable vibrations, but each method has its limitations. Recent studies on cable vibration control have demonstrated that semi-active dampers attached to stay cables may provide levels of damping far superior to their passive counterparts as well as can potentially achieve performance levels nearly the same as comparable active devices with few of the detractions. Johnson, *et al*. (2000) used a taut string model of in-plane cable vibration and developed a control-oriented model using a static deflection shape in a series expansion for the cable motion. Ni, *et al*. (2002) proposed neural network-based controllers for reducing the excessive vibration of sagged stay cables incorporated with MR fluid dampers. Johnson, *et al*. (2003) extended their previous work by adding sag and inclination to the cable model, and showed that the response of the cable was significantly reduced by semi-active dampers for a wide range of cable sag and damper locations. Also, Christenson (2001) experimentally verified the effectiveness of MR fluid damper-based semi-active control technology. However, most of the previous numerical and experimental studies considered only one specific semi-active control algorithm, such as the clipped-optimal control algorithm and the neural network-based control algorithm, in which they are interested.

In this paper, the effectiveness of a smart damping system using an MR fluid damper in mitigating cable responses is systematically investigated by considering the four commonly used semi-active control strategies, such as the control based on Lyapunov stability theory (Leitmann 1994), the maximum energy dissipation (McClamroch and Gavin 1995, Choi, *et al*. 2007b), the clipped optimal control (Dyke, *et al*. 1996) and the modulated homogeneous friction algorithms (Inaudi 1997). Numerical simulation considers a stay cable excited by external load distributed along the cable and controlled by an MR fluid damper. The control performance of each semi-active control algorithm has been compared with those of the passive-type control systems employing an MR fluid damper.

2. Cable dynamics

Stay cables typically have small sag (1 % sag-to-length ratio or less) with high tension-to-weight ratios. With small sag, the motion of the cable may be modeled by the motion of a taut string (Irvine 1981). Therefore, the transverse motion of the cable with a semi-active damper attached transverse to the cable is depicted as shown in Fig. 1, where $v(x, t)$ is the transverse deflection of the cable, L is the length of cable, x_d is the location of the damper, $F_d(t)$ is the damper force, T is the cable tension, m is the cable mass per unit length and ς is the modal damping ratio.

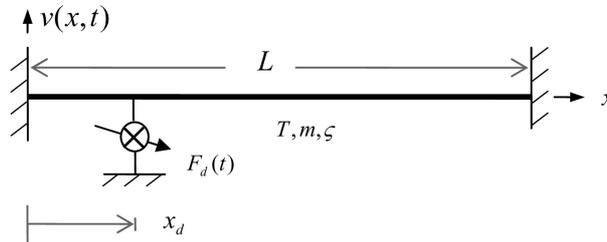The motion of the taut cable in the linear range is described by the following partial differential equation,

Fig. 1 Cable with attached semi-active damper

$$m\ddot{v}(x, t) + c\dot{v}(x, t) - Tv''(x, t) = f(x, t) + F_d(t)\delta(x - x_d)$$ (1)

where $f(x, t)$ is the external load and c is the cable viscous damping per unit length.

It is assumed that the transverse deflection may be approximated using finite series as

$$v(x, t) = \sum_{j=1}^{n} \phi_j(x)\eta_j(t)$$ (2)

where n is the number of modes considered, $\eta_j(t)$ is the generalized displacement and $\phi_j(x)$ is a shape function.

Several hundred terms in the sine series are usually used as shape functions, even though it takes considerable computation effort. However, when trying to use active or semi-active control, controllers with such complexity can cause various problems in the control design and implementation stages. Johnson, *et al*. (2000) showed that introducing shape function (Eq. 3) based on the deflection due to a static force at the damper location can reduce the number of terms required for the comparable accuracy. Fig. 2 shows a simple approximation of the first damped eigenfunction using a linear combination of the static deflection shape and the first sine term. The static deflection shape function is shown in Fig. 2(b) and is given by

$$\phi_1(x) = \begin{cases} x/x & 0 \leq x \leq x_d \\ (L-x)/(L-x_d) & x_d \leq x \leq L \end{cases}$$ (3)

The other shape functions remain sinusoidal as follows:

$$\phi_{j+1}(x) = \sin \pi j \frac{x}{L} \qquad j = 1, 2 \ldots n - 1$$ (4)

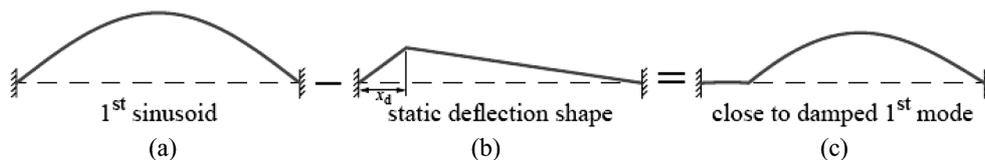We can get the equation of motion written in matrix form from a standard Galerkin approach as

Fig. 2 Simple approximation of first damped eigenfunction (Johnson, *et al*. 2000)

$$M\ddot{\eta}(t) + C\dot{\eta}(t) + K\eta(t) = f(t) + \varphi F_d(t) \tag{5}$$

resulting in the ($n \times n$) mass matrix M,

$$M = [m_{ij}], m_{ij} = m\int_0^L \phi_i(x)\phi_j(x)dx \tag{6}$$

the ($n \times n$) stiffness matrix K,

$$K = [k_{ij}], k_{ij} = -T\int_0^L \phi_i'(x)\phi_j'(x)dx \tag{7}$$

the ($n \times 1$) load vector f,

$$f = [f_i], f_i = \int_0^L f(x, t)\phi_i(x)dx \tag{8}$$

and the ($n \times 1$) damper force vector φ,

$$\varphi = \phi(x_d) = [\phi_1(x_d) \ \phi_2(x_d) \dots \phi_n(x_d)]^T \tag{9}$$

And the damping matrix C can be derived from mass, stiffness matrices and the given set of modal damping ratios.

Eq. (5) can be written in state-space form as

$$\dot{z} = Az + BF_d(t) + Gf \tag{10}$$

$$Z = C_Z z + D_Z F_d(t) + H_Z f \tag{11}$$

$$y = C_y z + D_y F_d(t) + H_y f + v \tag{12}$$

where $z = [\eta \ \dot{\eta}]^T$ is the ($2n \times 1$) state vector, $Z = [\eta \ \dot{\eta} \ \ddot{\eta}]^T$ is a ($3n \times 1$) vector of quantities to be regulated, y is a ($2 \times 2n$) vector of noisy sensor measurements, v is a (2×1) vector of stochastic sensor noise processes, and matrices are

$$A = \begin{bmatrix} 0 & I \\ -M^{-1}K & -M^{-1}C \end{bmatrix} \quad B = \begin{bmatrix} 0 \\ M^{-1}\varphi \end{bmatrix} \quad G = \begin{bmatrix} 0 \\ M^{-1} \end{bmatrix}$$

$$C_Z = \begin{bmatrix} I & 0 \\ 0 & I \\ -M^{-1}K & -M^{-1}C \end{bmatrix} \quad D_Z = \begin{bmatrix} 0 \\ 0 \\ M^{-1}\varphi \end{bmatrix} \quad H_Z = \begin{bmatrix} 0 \\ 0 \\ M^{-1} \end{bmatrix}$$

$$C_y = \begin{bmatrix} \varphi^T & 0 \\ -\varphi^T M^{-1}K & -\varphi^T M^{-1}C \end{bmatrix} \quad D_y = \begin{bmatrix} 0 \\ \varphi^T M^{-1}\varphi \end{bmatrix} \quad H_y = \begin{bmatrix} 0 \\ \varphi^T M^{-1} \end{bmatrix}$$

An observer for state estimation should be provided for state feedback, since measurements are assumed to be available only at the damper location in the numerical example. A Kalman-Bucy filter is used as the observer for state estimation. The displacement and velocity are measured for inputs of the Kalman-Bucy filter, and then the state estimation vector $\hat{z} = [\hat{\eta} \ \dot{\hat{\eta}}]^T$ can be obtained from

$$\dot{\hat{z}} = (A - L_{kf}C_y)\hat{z} + [L_{kf} \ \ B - L_{kf}D_y \ \ G - L_{kf}H_y] \begin{Bmatrix} y \\ F_d(t) \\ f \end{Bmatrix} \qquad (13)$$

$$\begin{bmatrix} \hat{y} \\ \hat{z} \end{bmatrix} = \begin{bmatrix} C_y \\ I \end{bmatrix} \hat{z} + \begin{bmatrix} 0 & D_y & H_y \\ 0 & 0 & 0 \end{bmatrix} \begin{Bmatrix} y \\ F_d(t) \\ f \end{Bmatrix} \qquad (14)$$

where L_{kf} is the estimator gain obtained by solving an algebraic Riccati equation (Burl 1999).

3. Semi-active MR fluid damper

As many researches verified the efficiency of the semi-active controller, various semi-active control devices such as variable orifice dampers, variable friction dampers, controllable tuned liquid dampers, and controllable fluid dampers have been developed rapidly. Semi-active devices are distinguished from active control devices in the fact that they can produce only dissipative force and different from passive control devices in the fact that characteristics of devices can be changed in real time. Controllable fluid dampers are similar with variable orifice dampers but it is different that controllable fluid dampers use controllable fluids such as electrorheological (ER) fluids and magnetorheological (MR) fluids and do not require a mechanical valve. Many studies on civil structural control using ER or MR fluids have proved the efficiency of those control systems recently.

The damping device considered in this study is an MR fluid (Carlson 1994), a kind of controllable fluid dampers using MR fluids. The simple dynamic model of an MR fluid damper has been developed by Terasawa, *et al.* (2004). They adopted the MR fluid damper (RD-1097-01) provided by Lord Corporation and the damping force $F_d(t)$ in their proposed dynamic model of the MR fluid damper can be expressed by

$$F_d = \sigma_a w + \sigma_0 w V + \sigma_1 \dot{w} + \sigma_2 \dot{v}_d + \sigma_b \dot{v}_d V \qquad (15)$$

$$\dot{w} = \dot{v}_d - a_0 |\dot{v}_d| w \qquad (16)$$

where $w(t)$ is the internal state variable (m), $v_d(t)$ is the displacement of cable at damper location (m), $V(t)$ is the input voltage to the MR fluid damper, σ_0 is the stiffness of $w(t)$ influenced by $V(t)$ (N/(mV)), σ_1 is the damping coefficient of $w(t)$ (Ns/m), σ_2 is the viscous damping coefficient (Ns/m), σ_a is the stiffness of $w(t)$ (N/m), σ_b is the viscous damping coefficient influenced by $V(t)$ (Ns/(mV)), and a_0 is the constant value (1/m).

4. Semi-active control algorithms for cable vibration

Various approaches have been proposed for the control of semi-active devices. Since the response of the semi-active device is dependent on deformation of the device as well as the command input, it is not possible to command directly to generate a specified damper force. Instead, the value of the voltage applied to the current driver is changed to increase or decrease the damper force. Based on this observation, semi-active control algorithms are designed to produce the command voltage input.

In this study, the commonly used four control algorithms are adopted and evaluated through numerical simulation: the control algorithm based on the Lyapunov stability theory, the maximum energy dissipation algorithm, the clipped optimal control algorithm, and the modulated homogeneous friction algorithm. Detailed information of each control algorithm can be found in Jansen and Dyke (2000).

4.1. Control algorithm based on Lyapunov stability theory

According to the Lyapunov stability theory, the state is stable in the sense of Lyapunov when the rate of change of the Lyapunov function is negative semi-definite. Lyapunov's direct approach was applied to design a semi-active controller by Leitmann (1994). In this approach, the goal of the control law is to choose control inputs that will result in making the following rate of change of the Lyapunov function as possible:

$$\dot{V}_L = -\frac{1}{2}z^T Q_P z + z^T P_L B F_d + z^T P_L G f \tag{17}$$

where z is the state vector, and P_L is the real, symmetric, positive definite matrix satisfying the following Lyapunov equation

$$A P_L + P_L A^T = -Q_P \tag{18}$$

for a positive semi-definite matrix Q_P.

The only term in Eq. (17) which can be directly affected by a change in the control voltage is the middle term which contains the force vector F_d. Thus, the control law which will minimize $\dot{V}_L$ is

$$V = V_{\max} H((-z)^T P_L B F_d) \tag{19}$$

where $V_{\max}$ is the maximum voltage input to an MR fluid damper, and $H(\cdot)$ is the heaviside step function.

4.2. Maximum energy dissipation algorithm

The maximum energy dissipation algorithm was presented as a variation of the decentralized bang-bang approach by McClamroch and Gavin (1995). In the maximum energy dissipation algorithm, the Lyapunov function was chosen to represent the relative total vibratory energy in the system as (Jansen and Dyke 2000)

$$V_L = \frac{1}{2}\eta^T K \eta + \frac{1}{2}\dot{\eta}^T K \dot{\eta} \tag{20}$$

Calculating the rate of change of the Lyapunov function from Eq. (20), the term which can be directly affected by changes in the control voltage is identified and the control law for semi-active controller attached to cable is obtained as

$$V = V_{\max} H(-\dot{\eta}\, \varphi F_d) \tag{21}$$

This control algorithm commands the maximum control voltage when the cable system dissipates energy.

4.3. Clipped-optimal control algorithm

The clipped optimal control algorithm proposed by Dyke, *et al.* (1996) is the one that has been shown to be effective for use with the MR damper. This algorithm consists of two parts of controller. The primary controller is the LQR control design which gives the optimal control force, $F_{d_{ci}}$, that minimizes the cost function. In this study, LQR controller which is designed by Johnson, *et al.* (2000) and proved to perform well for stay cables is adapted. This controller uses force proportional to an estimate of the state of the system using feedback gain that minimizes the cost function

$$J = \lim_{T \to \infty} E\left[\frac{1}{T}\int_0^T (z^T Q z + R F_{d_{ci}}^2)\,dt\right] \tag{22}$$

where Q and R is the response and control weighting matrices, respectively.

Optimal control force $F_{d_{ci}}$ is given by equation $F_{d_{ci}} = -Lz$ and the feedback gain L is given by the equation,

$$L = (R + D_Z^T Q D_Z)^{-1}(B^T P_c + D_Z^T Q D_Z) \tag{23}$$

where P_c satisfies the algebraic Riccati equation

$$A^T P_c + P_c A - (P_c B + C_Z^T Q D_Z)(R + D_Z^T Q D_Z)^{-1}(B^T P_c + D_Z^T Q D_Z) = -C_Z^T Q D_Z \tag{24}$$

The secondary controller, which accounts for the characteristics of MR fluid dampers that can only exert dissipative forces, is given by

$$V = V_{\max} H(\{F_{d_{ci}} - F_d\}F_d) \tag{25}$$

The control law means that when the force produced by the damper is smaller than the desired optimal force and the two forces have the same direction, the controller will command the maximum voltage to control device.

4.4. Modulated homogeneous friction algorithm

The modulated homogeneous friction algorithm was originally proposed for the controller using a variable fiction damper (Inaudi 1997), but it can be adopted for an MR fluid damper because there are strong similarities between the behavior of a variable friction device and the MR fluid damper. This

algorithm commands more slip force with damper deformation larger by increasing the damping coefficient to improve the energy dissipation process of semi-active dampers. In this approach, at every local extreme deformation of the device the desired control force F_{d_n} can be determined as

$$F_{d_n} = g_n[P[v_d(t)]] \tag{26}$$

where g_n is the positive gain, the operator $P[\cdot]$ is defined as

$$P[\Delta_i(t)] = \Delta_i(t-s) \tag{27}$$

for $s = \{\min x \geq 0 | \dot{\Delta}_i(t-x) = 0\}$ and $\Delta_i(t-s)$ is the most recent local extreme deformation of the device.

Because the force produced by the MR fluid damper cannot be directly commanded as in the clipped optimal control law, the force level, or the command voltage input to dampers is renewed as following equations

$$V = V_{\max}H(\{F_{d_n} - |F_d|\}) \tag{28}$$

5. Numerical simulation

5.1. Numerical models of cable damping model

To numerically evaluate several semi-active control algorithms for an MR fluid damper-based smart damping systems of cable vibration, a numerical model was extracted from the real-scaled PVC covered high-tension cable as shown in Fig. 3. The cross section and properties of the cable are demonstrated in Fig. 4 and Table 1. In the table, l is the length of the cable, m is the cable mass per unit length, E is the modulus of elasticity, EI and EA are the flexural and axial rigidity respectively, T is the cable tension, and ς is the modal damping ratio.
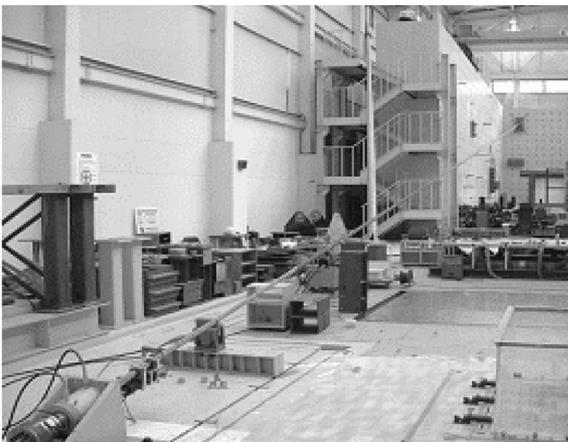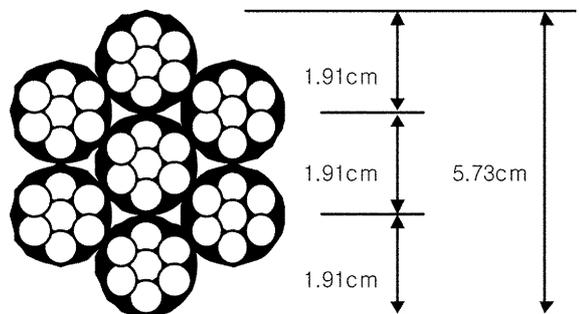

Fig. 3 Real-scaled stay cable

Fig. 4 Cross section of the cable

Table 1 Cable characteristics

Parameter	Value	Parameter	Value
l	44.7 m	m	89.86 kg/m
E	1.89×10^8 kN/m^2	EI	3.79×10^5 kNm^2
T	500 kN	EA	77.36 kN
ς	$\varsigma_1 = 0.0015$ $\varsigma_{i \geq 1} = 0.0005$		

Table 2 Parameters for damper model

Parameter	Value	Parameter	Value
σ_0 (N/(mV))	28815 MF	σ_a (N/m)	30542 MF
σ_1 (Ns/m)	0.131 MF	σ_b (Ns/(mV))	16.3 MF
σ_2 (Ns/m)	29.6 MF	σ_0 (V/N)	3198

The MR fluid damper is constructed to provide controllable damping forces and the parameters identified by Terasawa, *et al*. (2004) are in Table 2. This damper has a maximum force level of approximately $\pm 2000N$ and maximum voltage input $V_{max} = 10$ volts. In the table, MF represents the magnification factor (MF = 10 in this numerical simulation).

The MR fluid damper is positioned at 3.129 m (7% of the cable length) from the bottom support and it provides in-plane forces transverse to the cable.

5.2. Evaluation criteria

The four control algorithms considered in this study are evaluated using a set of the evaluation criteria. The first and second evaluation criteria are measurements of the displacement at mid-span and quarter-span, respectively. The third and forth evaluation criteria are root mean square (RMS) of cable deflection and velocity. Each evaluation criterion is normalized by the uncontrolled value. All the evaluation criteria are defined by

$$J_1 = \frac{\max(v_{midspan}(t))}{\max(v_{midspan}(t))\big|_{uncontrolled}} \tag{29}$$

$$J_2 = \frac{\max(v_{quarterspan}(t))}{\max(v_{quarterspan}(t))\big|_{uncontrolled}} \tag{30}$$

$$J_3 = \frac{\sigma^2_{displacement}(t)}{\sigma^2_{displacement}(t)\big|_{uncontrolled}} \tag{31}$$

where $$\sigma^2_{displacement}(t) = E[\int_0^L v^2(x,t)dx] = \frac{1}{m}trace\{M^{1/2}E[\eta(t)\eta^T(t)]M^{1/2}\} \tag{32}$$

$$J_4 = \frac{\sigma^2_{velocity}(t)}{\sigma^2_{velocity}(t)\big|_{uncontrolled}} \tag{33}$$

where
$$\sigma^2_{velocity}(t) \;=\; E[\int_0^L \dot{v}^2(x,t)dx] \;=\; \frac{1}{m} trace\{M^{1/2}E[\dot{\eta}(t)\dot{\eta}^T(t)]M^{1/2}\} \tag{34}$$

5.3. External load

It has been reported that the response of a stay cable under wind loads tends to be dominated by the first few modes. In this study, therefore, the excitation is assumed to be a subset of the series in equation (4) using one term

$$f(x,y) \;=\; W(t)\sin\pi\frac{x}{L} \tag{35}$$

where $W(t)$ is a zero-mean Gaussian white noise process with $E[W(t)W(t+\tau)]=\delta(\tau)$. If a damper is not employed to a cable, the response would be dominated only by its first mode.

5.4. Numerical results

A series of numerical simulations were conducted. 20 shape functions are used in all the simulations. To compare the performance of the smart damping systems employing several semi-active control algorithms to that of comparable passive systems, two cases are considered in which the MR fluid dampers are used in a passive mode by maintaining a constant voltage to the devices: passive off ($V=0$ volts) and passive on ($V=10$ volts). For all the semi-active control algorithms considered except the maximum energy dissipation algorithm (MED), the optimal parameters for each controller should be obtained to make the well-performed controller. In the case of the control algorithm based on the Lyapunov stability theory (LYAP), the several tries are carried out by varying the values in Q_p because of no standard method for selecting Q_p. The resulting Q_p is the identity matrix. In the case of the clipped

optimal control algorithm (CO), after varying weight R from 10^3 to 10^{-12} with the fixed $Q = \begin{bmatrix} \frac{1}{2}M & 0 \\ 0 & \frac{1}{2}M \end{bmatrix}$, the

optimal control weighting matrix is obtained as $R=10^{-11}$. In the case of the modulated homogeneous friction algorithm (MHF), the optimal gain $g_n=50,000$ N/m is selected after several numerical simulations.

Numerical simulations of the two cases have been carried out. In the first case (Case 1), the relatively large wind load is considered, and the other case (Case 2), the excitation with one-third magnitude is considered to investigate the adaptability with respect to the change in the magnitude of the excitation. Fig. 5 shows that the time history response of generated wind load for Case 1 and Case 2, respectively. In Case 1, the uncontrolled maximum displacements at mid-span and at quarter-span are 29.62 cm and 20.94 cm, respectively. In Case 2, on the other hand, those values are 9.87 cm and 6.98 cm, respectively.

Table 3 and Fig. 6 show the normalized responses of control algorithms with respect to the uncontrolled system. As shown in the table and the figure, all the control algorithms including passive-on and passive-off significantly reduce the responses compared with the uncontrolled system. In the passively operated systems, the performance of the passive-on is much better than that of the passive-off system. Of all the semi-active control algorithms, the clipped optimal control algorithm and the modulated homogeneous algorithm are slightly better than the other two algorithms that are comparable to the passive on system. Although the performance of the clipped optimal control algorithm gives a little superior than that of the MHF, the latter may be promising to achieve the good performance to cable
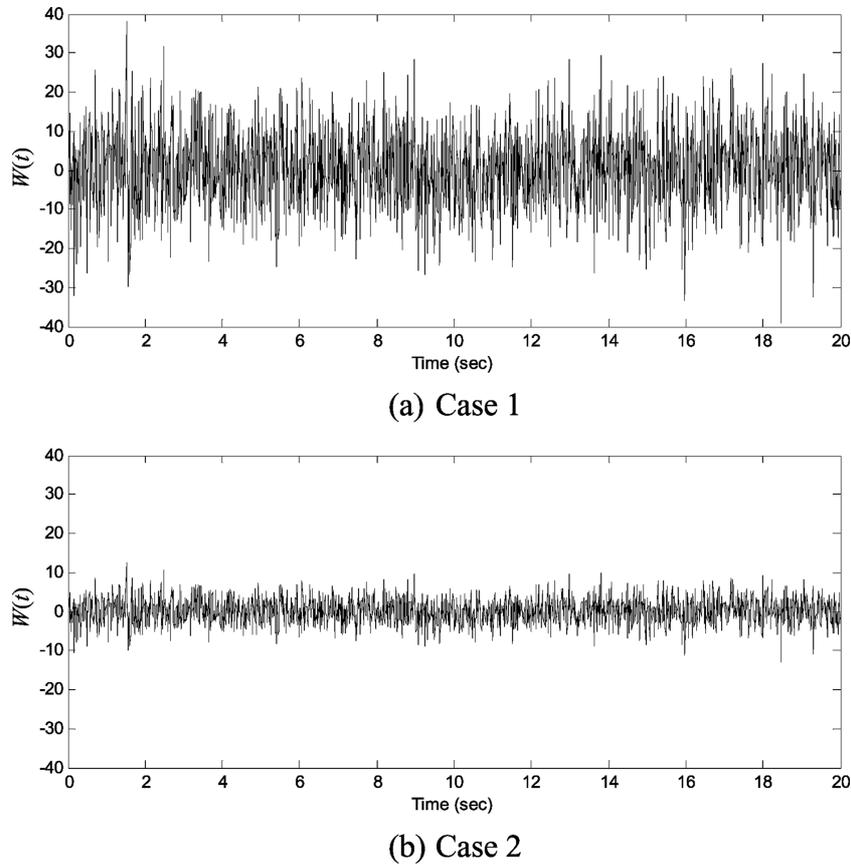
(a) Case 1

(b) Case 2

Fig. 5 Zero-mean gaussian white noise $W(t)$

Table 3 Normalized responses with respect to the uncontrolled system (Case 1)

Control algorithms	Passive-off	Passive-on	LYAP	MED	CO	MHF
J_1 (max. displ. at mid-span)	0.4203	0.2326	0.2215	0.2316	0.1918	0.1935
J_2 (max. displ. at quarter-span)	0.4078	0.2479	0.2283	0.2455	0.1891	0.2063
J_3 (RMS displ.)	0.3605	0.2090	0.1785	0.2047	0.1412	0.1611
J_4 (RMS velocity)	0.3617	0.2249	0.1884	0.2197	0.1527	0.1700

structure because of its simplicity.

Table 4 shows the max and RMS control forces of each control algorithm. The clipped optimal control algorithm, one of the most efficient control algorithms used 458.6 N RMS damper force, which is most smallest in the all algorithms.

The numerical simulation results of Case 2 are demonstrated in Table 5 and Fig. 7. In this case that the magnitude of the excitation is one third in Case 1, the performance of the passive-off system is clearly better than that of the passive-on system. This shows the lack of the adaptability of the passive-type control system. On the other hand, all the semi-active control algorithms except the maximum energy dissipation algorithm show the good control performance. The clipped optimal control and the
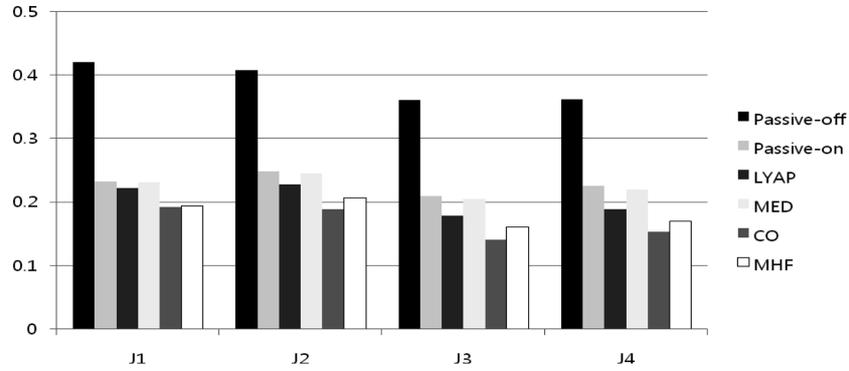
Fig. 6 responses with respect to the uncontrolled system (Case 1)

Table 4 Control forces of each control algorithm (Case 1)

Control algorithms	Passive-off	Passive-on	LYAP	MED	CO	MHF
Max. control force	240.15	1439.2	1821.1	1452.0	1858.4	1478.6
RMS control force	123.34	754.75	506.82	759.77	458.6	517.4

Table 5 Normalized responses with respect to the uncontrolled system (Case 2)

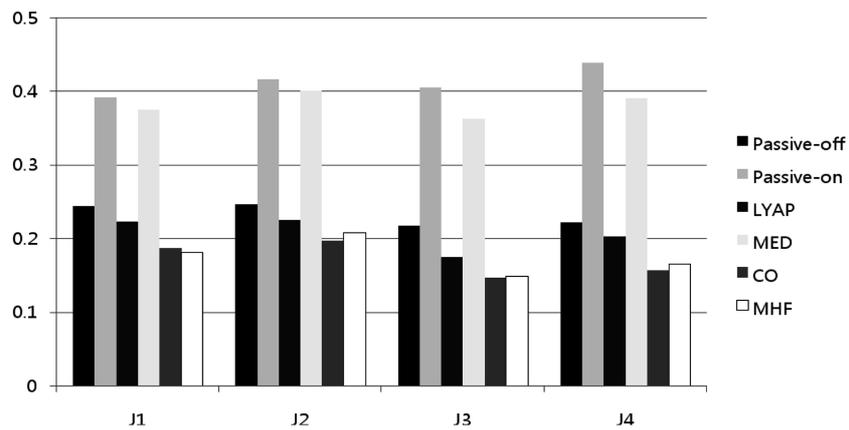| Control algorithms	Passive-off	Passive-on	LYAP	MED	CO	MHF
J_1 (max. displ. at mid-span)	0.2442	0.3921	0.2229	0.3749	0.1874	0.1814
J_2 (max. displ. at quarter-span)	0.2464	0.4169	0.2249	0.4011	0.1977	0.2077
J_3 (RMS displ.)	0.2175	0.4054	0.1750	0.3628	0.1470	0.1484
J_4 (RMS velocity)	0.2216	0.4388	0.2026	0.3908	0.1570	0.1656

Fig. 7 responses with respect to the uncontrolled system (Case 2)

modulated homogeneous friction algorithms show the better performance than other algorithms similar to Case 1. In the case of the maximum energy dissipation algorithm, its performance in Case 2 is poor while that in Case 1 is relatively good. That might be because it is less adaptable to the intensity change

Table 6 Control forces of each control algorithm (Case 2)

Control algorithms	Passive-off	Passive-on	LYAP	MED	CO	MHF
Max. control force (N)	123.59	1147.0	1376.3	1120.7	1338.1	1128.1
RMS control force (N)	82.12	542.90	251.17	516.39	176.46	195.0

of the excitation than other semiactive control algorithm such as the clipped optimal control algorithm because of its simplicity. Table 6 shows the max and RMS damper force of each control algorithm. The tendency is almost same with the results of Case 1.

6. Conclusions

In this study, the efficacy of an MR fluid damper-based smart damping systems for vibration suppression of stay cables has been analytically investigated. The four commonly used semi-active control algorithms, such as the control based on Lyapunov stability theory, the maximum energy dissipation, clipped optimal control, and the modulated homogeneous friction algorithm, are applied to smart damping systems for the stay cable, and the performance of each one is numerically evaluated. It is verified from the numerical simulation results that all the semi-active control algorithms has a good control performance to mitigate cable vibration. Especially, the clipped optimal control and the modulated homogeneous friction algorithm are superior to other control algorithms. In addition, the results of the passively operated systems clearly show that they do not have the adaptability to the intensity change of excitation. Therefore, the MR fluid damper-based smart damping systems adopting the semi-active control algorithm such as the clipped optimal control algorithm and the modulated homogeneous friction algorithm could be considered as one of the promising strategy for vibration mitigation of stay cables.

Acknowledgements

References

Burl, J. B. (1999), *Linear Optimal Control*, Addison Wesley Longman, Inc., Menlo Park, California.
Christenson, R. E. (2001), "Semiactive control of civil structures for natural hazard mitigation: analytical and experimental studies", Ph.D. Dissertation, Department of Civil Engineering and Geological Sciences, University of Notre Dame, Indiana.
Carlson, J. D., The promise of controllable fluids, Proceeding of Actuator 94, AXON Technologies Consult GmbH, 266-270.
Cho, S. W., Jung, H. J. and Lee, I. W. (2005), "Smart passive system based on magnetorheological damper",

Smart Mater. Struct., **14**, 707-714.

Choi, K. M., Jung, H. J., Cho, S. W. and Lee, I. W. (2007a), "Application of smart passive damping system using MR damper to highway bridge structure", *J. Mech. Sci. Tech.*, **21**, 870-874.

Choi, K. M., Lee, H. J., Cho, S. W. and Lee, I. W. (2007b), "Modified energy dissipation algorithm for seismic structures using magnetorheological damper", *KSCE J. Civil Eng.*, **11**(2), 121-126.

Dyke, S. J., Spencer, Jr., B. F., Sain, M. K. and Carlson, J. D. (1996), "Modeling and control of magnetorheological dampers for seismic response reduction", *Smart Mater. Struct.*, **5**, 565-575.

Fu, Y., Dyke, S. J. and Caicedo, J. M. (1999), "Seismic response control using smart dampers", *Proceeding of the 1999 American Control Conference*, San Diego, California, June 2-4.

Inaudi, J. A. (1997), "Modulated homogeneous friction: a semi-active damping strategy", *Earthq. Eng. Struct. Dyn.*, **26**(3), 361-376.

Irvine, H. M. (1981), *Cable Structures*, MIT Press, Cambridge, Massachusetts.

Jansen, L. M. and Dyke, S. J. (2000), "Semiactive control strategies for MR dampers: comparative study", *J. Eng. Mech.*, ASCE, **126**(8), 795-803.

Johnson, E. A., Baker, G. A., Spencer, Jr. B. F. and Fujino, Y. (2000), "Mitigating stay cable oscillation using semiactive damping, Smart Structures and Materials 2000: Smart Systems for Bridges, Structures, and Highways", *Proceedings of SPIE*, **3988**, 207-216.

Johnson, E. A., Christenson, R. E. and Spencer, Jr., B. F. (2003), "Semiactive damping of cables with sag", *Computer-aided Civil and Inf. Eng.*, **18**(2), 132-146.

Jung, H. J., Choi, K. M., Park, K. S. and Cho, S. W. (2007), "Seismic protection of base isolated structures using smart passive control system", *Smart Struct. Sys.*, **3**(3), 385-403.

Leitmann, G. (1994), "Semiactive control for vibration attenuation", *J. Intell. Mater. Sys. Struct.*, **5**, 841-846.

McClamroch, N. H. and Gavin, H. P. (1995), "Closed loop structural control using electrorheological damper", *Proceeding of the American Control Conference*, Seattle, Washington, 4173-4177.

Ni, Y. Q., Chen, Y., Ko, J. M. and Cao, D. Q., "Neuro-control of cable vibration using semi-active magneto-rheological dampers", *Eng. Struct.*, **24**(3), 295-307.

Spencer, Jr., B. F., Dyke, S. J., Sain, M. K. and Carlson, D. J. (1997), "Phenomenological model of magnetorheological damper", *J. Eng.*, ASCE, **123**(3), 230-238.

Terasawa, T. and Sakai, C. (2004), "Adaptive identification of MR damper for vibration control", *Proceedings of 43rd IEEE Conference on Decision and Control*, 2297-2303.

Yang, J. N., Agrawal, A. K., Samali, B. and Wu, J. C. (2004), "Benchmark problem for response control of wind-excited tall buildings", *J. Eng. Mech.*, ASCE, **130**(4), 437-446.